



Highly conductive, flexible and functional multi-channel graphene microtube fabricated by electrospray deposition technique

He Gong¹, Meng-Fei Li¹, Jun-Xiang Yan¹, Miao-Ling Lin², Xue-Lu Liu², Bin Sun¹, Ping-Heng Tan², Yun-Ze Long¹, and Wen-Peng Han^{1,3,*}

¹ College of Physics, Qingdao University, Qingdao 266071, China

² State Key Laboratory of Superlattices and Microstructures, Institute of Semiconductors, Chinese Academy of Sciences, Beijing 100083, China

³ State Key Laboratory of Bio-Fibers and Eco-Textiles, Qingdao University, Qingdao 266071, China

Received: 10 June 2019

Accepted: 13 August 2019

Published online:
19 August 2019

© Springer Science+Business
Media, LLC, part of Springer
Nature 2019

ABSTRACT

Highly conductive and flexible graphene-based microtubes (μ -GTs) have many potential applications in catalyst supports and wearable electronics. However, there is a lack of effective method to fabricate the high-performance μ -GTs, especially the multi-channel ones. In this work, the electrostatic spray deposition technique was introduced to fabricate the graphene oxide-coated polyester thread from cost-efficient graphene oxide suspensions. After the polyester thread template was removed along with the reduction of graphene oxide by thermal annealing, the multi-channel μ -GT was prepared successfully. Due to the multiple structure of the cross section and the vertically aligned reduced graphene oxide sheets of the tube wall, the multi-channel μ -GT exhibits many excellent properties, such as highly conductive, good flexibility, and functionalization. For example, the electrical conductivity of the multi-channel μ -GT thermally reduced at 1200 °C is about $1.99 \times 10^4 \text{ S m}^{-1}$ at room temperature and can light a LED as a conductive wire. And the electrical conductivity is nearly invariable in either the straight or bent state though a cyclic bending test up to 800 times. In addition, the TiO_2 /multi-channel μ -GT composite shows strong photocurrent response in which the multi-channel μ -GT provides a super platform due to the high specific surface area. The high-performance μ -GTs obtained by the simple method opens the immense potentials for application in wearable devices.

He Gong and Meng-Fei Li contributed equally to this work.

Address correspondence to E-mail: han_wenpeng@163.com; wphan@qdu.edu.cn

Introduction

Because of the high electrical and thermal conductivities, excellent mechanical properties, and large specific surface area [1–4], graphene has gained a wide attention as a two-dimensional (2-D) carbon nanomaterial. Nevertheless, to realize its practical application, the sheet-like tiny flakes must be assembled into the macroscopic superstructures with their inherent attributes be maintained. To this end, a number of effective studies have been done on the fabrication of 1-D macroscopic fibers [5–7], 2-D macroscopic configurations [8–13] and 3-D frameworks [14–17]. Because the ease of functionalization as well as retains the characteristics of traditional fibers, a rich family of graphene-based fibers have been developed and promising multifunctional in many fields [18–29]. Among them, graphene-based microtube (μ -GT) as one kind of special graphene-based fiber has shown many potential applications in catalyst supports, wearable electronics, purification, and sensing due to their large specific surface area, good conductive performance and excellent mechanical behavior [26–29].

Some traditional manufacturing methods including wet-spinning [7, 20–22] and dry-spinning [25] have been used to fabricate the solid graphene-based fibers. In particular, Gao et al. [22] have recently presented a new industrially scalable strategy based on wet-spinning to produce graphene fibers with excellent performance characteristics. However, the usual approach is not suitable for the preparation of μ -GTs because of its special morphologies. Until now just several techniques have been successfully developed to prepare μ -GTs, e.g., coaxial spinning [26], chemical vapor deposition [27], hydrothermal synthesis [29], and electrochemical deposition technique [28]. Among these methods, the template is an essential part as a core for the formation of tubular structure during the fabricating process. The difference between these methods is the selection of the templates. For the coaxial spinning method, soft template (methanol solution) was used as the core, which could be easily removed in the drying process of graphene oxide (GO) microtube. But the spinning conditions including both the feeding rates and the concentration of solution need to be precisely controlled in the spinning process [26]. Cu wire as the hard template was usually used in the other three

methods because of its high electrical conductivity and active catalytic property [27–29]. After etching the Cu wire by the FeCl_3 aqueous solution, the μ -GTs with the well tubular structure can be obtained. However, the etching process is time-consuming, commonly lasts 10 h [27–30]. In addition, the μ -GTs obtained from above methods usually possess only a single channel [26–28] or a few channels [29]. Compared with the multi-channel μ -GTs, such few-channel μ -GTs usually exhibit poor performance in the application of catalyst support and wearable electronics due to the smaller specific surface area and simple cross-sectional structure. Thus, the preparation of the μ -GTs, especially the multi-channel ones by using a simple and efficient method, has become an urgent problem in the future practical application.

In this work, the electrostatic spray deposition (ESD) technique was introduced to fabricate the GO-coated polyester thread from cost-efficient GO suspensions. After the reduction of GO sheets and disintegration of polyester thread in the thermal annealing process, the multi-channel μ -GTs were prepared successfully in the end. Interestingly, due to the multiple structure of the cross section and the vertically aligned reduced graphene oxide sheets of the tube wall, the as-prepared multi-channel μ -GTs exhibit good electrical conductivity, excellent flexibility, and functionalization, which promise great potential in application of wearable devices.

Materials and methods

Materials

Single-layer GO dispersion (N,N-dimethylformamide as solvent and single-layer rate more than 99.5%) were commercially obtained from Gaoxi Technology (Hangzhou, China), which have a concentration of 9 mg g^{-1} and average platelet diameter of 5–8 μm . Polyester thread was purchased from Verda (China), cleaned in ethanol with ultrasonic treatment for about 10 min and dried in air before used for preparing GO-coated polyester thread. The TiO_2 (P25) nanoparticles were purchased from Aladdin Industrial Corporation.

Fabrication of GO-coated polyester thread and μ -GTs

GO-coated polyester thread was fabricated by ESD setup as shown schematically in Fig. 1a. In typical GO-coated polyester thread fabrication processes, the GO solution was fed into syringe through a syringe pump at a feeding rate of $12 \mu\text{L min}^{-1}$, and a voltage of 8 kV was applied between the stainless steel nozzle (diameter 0.41 mm) and substrate. The distance of the stainless steel nozzle and the substrate was set to 3 cm. A home-made rectangular frame was entwined with polyester thread and then was placed on the substrate. The spacing between adjacent threads is approximately 1 mm (Fig. 1a). To ensure the polyester thread can be evenly coated by the GO sheets, the home-made rectangular frame should be overturned every 15 min during fabrication process.

The as-prepared GO-coated polyester thread was immersed into GaCl_2 (5 wt%) solution for 30 min to improve the strength [18, 45]. After that, the GO-coated polyester was transferred into deionized water bath to wash away the residual GaCl_2 solution. It was dried in a draught drying cabinet at 40°C for 20 min. In the end, the GO-coated polyester thread was thermally annealed in a tube furnace under Ar gas flow to reduce the GO sheets and remove the polyester thread. In the thermal reduced process, the samples were heated up from room temperature to various temperatures (600, 700, 800, 900, 1000, 1100, and 1200°C) at a rate of 4°C min^{-1} and kept at this temperature for 90 min to obtain multi-channel μ -GTs with different degrees of reduction.

The preparation of TiO_2/μ -GTs

TiO_2 nanoparticles (25 nm in diameter) were introduced into multi-channel μ -GTs by soaking them into commercial TiO_2 P25 aqueous suspension (12 mg mL^{-1}) for 30 min with slight stir. Subsequently the multi-channel μ -GTs were removed from suspension and dried in air at room temperature. Then TiO_2 -modified multi-channel μ -GTs were annealed in a tube furnace under Ar gas flow at 400°C for 30 min before photocurrent measurement.

Characterization

The morphology of the multi-channel μ -GTs was examined by scanning electron microscopies (FE-SEM, JSM-7500F), and the composition was characterized by X-ray photoelectron spectroscopy (XPS, Thermo, Escalab 250). Raman spectra were collected in the back-scattering geometry using a Jobin-Yvon HR Evolution micro-Raman system equipped with a liquid-nitrogen-cooled charge couple detector, a $100\times$ objective lens (numerical aperture ≈ 0.90), and a $600 \text{ lines mm}^{-1}$ grating. The excitation wavelength is 532 nm from a solid-state laser. Thermal gravimetric analysis (TGA, Mettler Toledo) was carried out under Ar purge at a heating rate of 5°C min^{-1} from room temperature to 800°C . The electrical resistance was tested using a four-probe technique on a physical property measurement system (Quantum Design, Quantum Design-EverCool II). The temperature dependence of the electric resistivity was investigated at temperatures from 10 to 300 K.

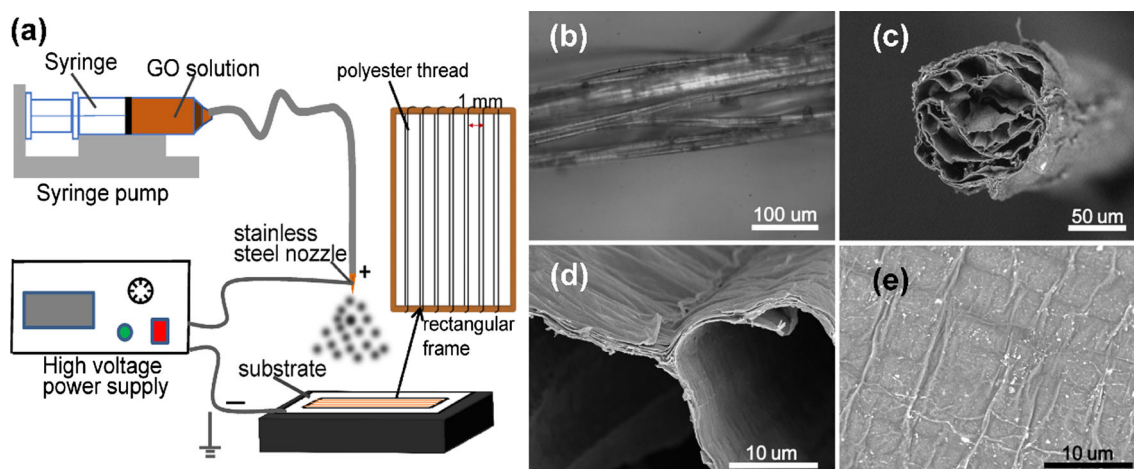


Figure 1 a Schematic illustration of the setup for fabricating of GO-coated polyester thread. b Optical images of loose polyester thread with many gaps. c SEM image of a μ -GT. d Cross-sectional SEM image of a multi-channel μ -GT. e SEM image of r-GOP (top view).

The bending tests on the resistance of multi-channel μ -GTs were carried out with a home-made two-point bending device, and the electrical resistance was recorded simultaneously by use of digital multimeter. For measuring the photocurrent response of TiO_2 -modified multi-channel μ -GTs, the current was recorded by electrochemical workstation (CHI760D, CH Instruments) upon exposure to a daylight lamp (40 W). The distance between the electrode and light source was 20 cm.

Results and discussion

In the regular preparation process of the μ -GTs, the key point is how to make the GO sheets uniformly deposited on the surface of the template and reduce the impact on properties and geometric shape of μ -GTs when removing the template in the end. The low-cost commercial polyester thread was selected as the template in this work, and GO sheets were homogeneous deposited on the polyester thread by using the ESD technique. After the GO sheets were reduced by thermal annealing along with the disintegration of polyester thread under high temperature, the multi-channel μ -GT was finally obtained as shown in Fig. 1c. The multi-channel μ -GTs have a higher specific surface area compared to the single-channel μ -GTs which is essential for a wide range of applications such as solid-state supercapacitor, highly efficient catalyst supports, and drug delivery. In addition, a characterized seamless structure was formed in the outside and inner surface of μ -GTs, because the reduced GO sheets flat overlap each other in the horizontal direction as shown in Fig. 1d. This is the key factor to form the channels rather than collapse after the template was removed. And what is probably more intriguing is that the tube wall of the μ -GT was constituted by many reduced GO sheets with obvious layer-by-layer structure which could be beneficial for improving the performance of the multi-channel μ -GTs. Besides, some obvious wrinkles can be found on the surface of the multi-channel μ -GT (Fig. 1e).

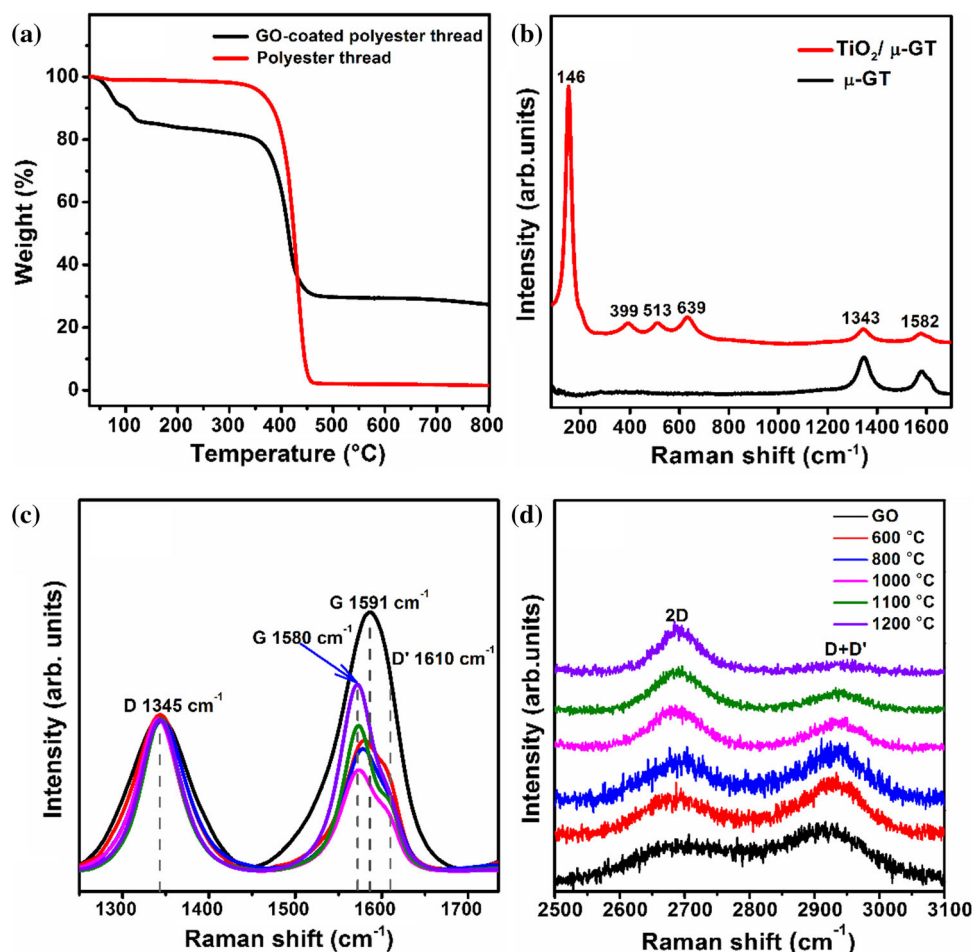
As a frequently used assembly technology of film materials, ESD has been extensively used in the preparation of graphene-based film materials recently [31–34]. However, the application of this technique on graphene-based fiber materials preparation has been reported rarely. In the electrospray

deposition process, the GO sheets had separated each other gradually in the spraying zone by the repulsive force due to same electric charges. Meanwhile, they fell toward the substrate due to the applied attractive force by electric field and the gravity of solution. With the help of the attractive force by applying electric field, the GO sheets can be easily deposited on the surface of the template. Thus, the materials of the template not only restrict to metallic materials such as Cu wire but also the low-cost commercial polyester thread used in this work. Furthermore, the polyester thread template can be removed along with the reduction process due to the low decomposition temperature of polyester thread (less than 460 °C, Fig. 2a). As the TGA curves shown in Fig. 2a, GO-coated polyester thread exhibited a slight weight loss around heating at about 100 °C due to evaporation of solvent and decomposition of oxygen-containing functional groups. When temperature was heated up to ~ 340 °C, both polyester thread and GO-coated polyester thread start to lose weight because of the decomposition of polyester. This process of weight loss continues to the temperature rise to nearly 460 °C. The polyester thread was totally disintegrated while the residual weight of GO-coated polyester thread is about 30% in the end. This indicates that the GO-coated polyester thread has transformed into a pure carbon-based material (μ -GTs) after high-temperature heat treatment above 500 °C.

On the other hand, the flexible geometrical structure of the commercial polyester thread promises possibility to produce multi-channel μ -GTs. The original polyester thread is composed of dozens of uniaxial arranged ultrafine yarns, and some gaps can be randomly formed between the yarns. By repeatedly tension and relaxation, the polyester thread can also show a loose structure with many gaps, as shown in Fig. 1b. The micron-sized GO sheets can be immersed into these gaps easily and were finally deposited onto the inner yarns. After the yarns were disintegrated at high temperature, numerous channels can be formed for μ -GTs (Fig. 1c).

To get information about structural changes of GO sheets after thermal reduction at different temperatures, which were investigated by the Raman spectroscopy. Representative Raman spectra of GO and multi-channel μ -GTs which were thermally reduced at 600, 800, 1000, 1100, and 1200 °C are shown in Fig. 2c, d. Because of the recovery of the hexagonal network of carbon atoms and the removal of

Figure 2 **a** TGA curves of GO-coated polyester thread and polyester thread. **b** Raman spectra of multi-channel μ -GT thermally reduced at 1100 °C and TiO₂/multi-channel μ -GT. **c** Raman spectra of GO and multi-channel μ -GTs thermally reduced at different temperatures; the intensities were normalized by the intensity of D mode of GO. **d** 2D modes of GO and multi-channel μ -GTs thermally reduced at different temperatures.

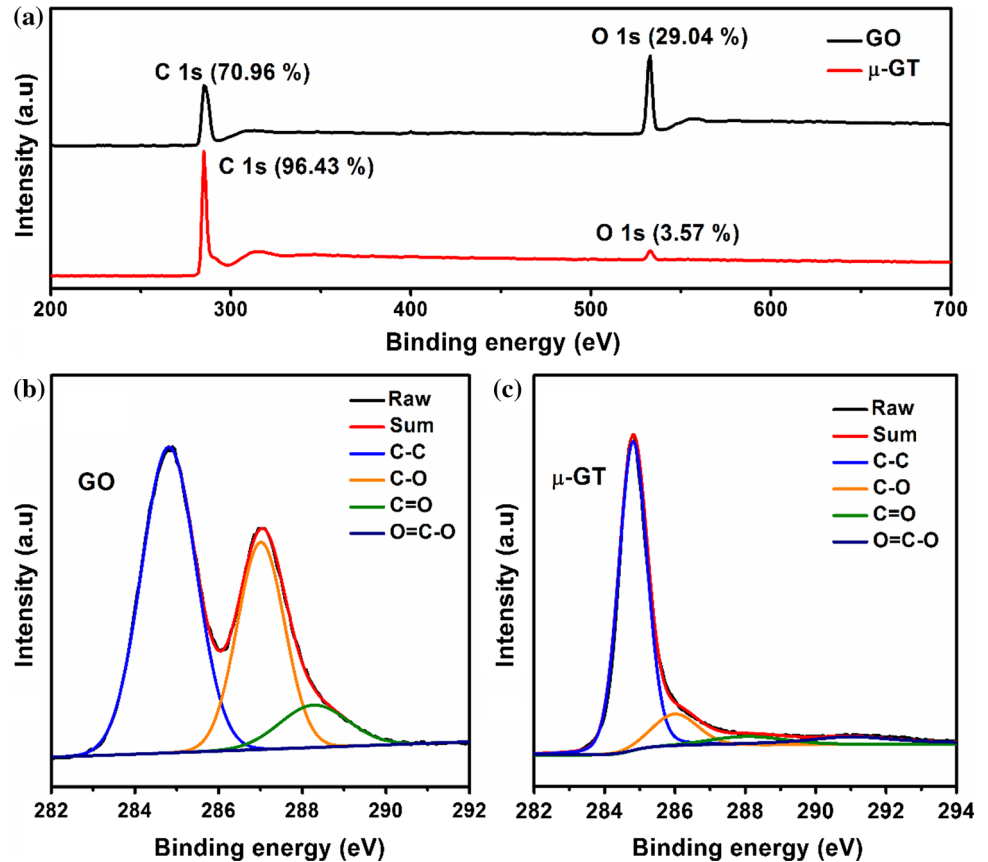


functional groups, the G peak down-shifts to 1580 cm^{-1} from 1591 cm^{-1} as well as the full width at half maximum of the D ($\sim 1345\text{ cm}^{-1}$) and G bands decrease down to values of $\sim 40\text{ cm}^{-1}$ after the thermal reduction process [35–37]. And the D' mode appears around 1610 cm^{-1} along with the G peak gets narrow enough by thermal annealing. Furthermore, the I_D/I_G ratio initially increases with reduction temperature increasing (lower than 1000 °C) and then decreases with further reduction. The initial increase of I_D/I_G ratio in reduced GO indicates that the reduction process below 1000 °C may alter the structure of GO (i.e., sp^2 carbon) which leads to increasing quantity of structural defects as reduction temperature increases. When the reduction temperature reaches above 1000 °C , the thermal reduction is mainly achieved through reducing the defects, which corresponds to the decreases of the I_D/I_G ratio [36, 37]. In addition, the Raman intensity of 2D band (2665 cm^{-1}) (Fig. 2d) increases obviously after

thermal annealing, further indicated that the recovery of sp^2 carbon in multi-channel μ -GTs [35–37].

The reduction in the amount of oxygen-containing functional groups of the GO sheets by thermal annealing also can be proved by measuring the C/O atomic ratio [38]. As the XPS spectra shown in Fig. 3a, the C/O atomic ratio increases to 27 after thermally reduced at 1200 °C that is more than 10 times to the GO. For further proving the oxygen-containing groups have been removed after thermal reduction, the high resolution C1 s peaks of the multi-channel μ -GTs have been studied. As shown in Fig. 3b, the XPS spectrum at the region of C1 s peak of the GO consists of three main parts which arising from C–C group ($\sim 284.7\text{ eV}$), C–O group ($\sim 287.1\text{ eV}$), and C=O group ($\sim 288.2\text{ eV}$), respectively, and one peripheral part arising from O=C–O group ($\sim 291\text{ eV}$) [38, 39]. After thermal reduction, the C–C bonds have become the only major part along with the majority of oxygen-containing groups in GO sheet

Figure 3 a XPS spectra of GO and multi-channel μ -GT thermally reduced at 1200 °C. XPS C1s peaks of b GO and c multi-channel μ -GT thermally reduced at 1200 °C.



(C–O, C=O, and O=C–O) are almost removed as shown in Fig. 3c.

The electrical properties of multi-channel μ -GTs will be enhanced along with the decrease of the content of functional groups and reforming of the crystallinity after thermal reduction process. To study the effects of reduction temperatures on electrical properties, the temperature-dependent resistivity of multi-channel μ -GTs thermally annealed at 600, 800, 1000, 1200 °C was measured. As shown in Fig. 4, the resistance increases with the temperature decreasing from 300 to 10 K, which indicates that the multi-channel μ -GTs are semiconductors. Interestingly, the resistivity was apparently decreased and the temperature dependence of the resistivity was gradually weakened along with the increase of the reduction temperature. These behaviors prove that the conductivity of the multi-channel μ -GTs can be improved by increasing the annealing temperature and turning from semiconductor into conducting characteristics gradually [6, 40]. Owing to the highly vertically aligned reduced GO sheets which built by ESD technique and the decrease of the content of

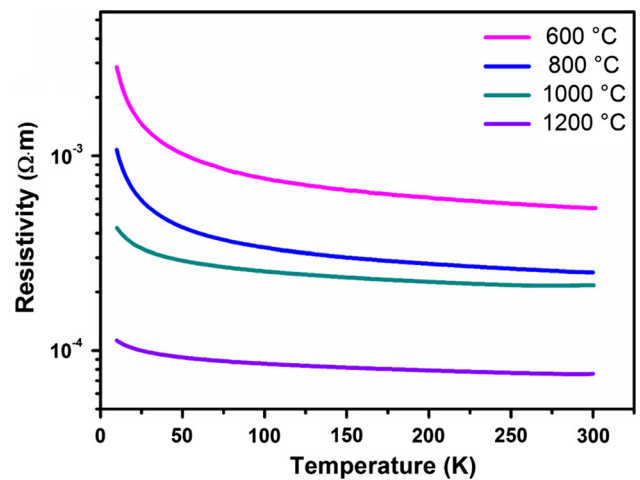


Figure 4 Temperature-dependent resistivity of thermally reduced multi-channel μ -GTs in the temperature range of 10 K to 300 K.

functional groups and reforming of the crystallinity by thermal annealing, the electrical conductivity of the multi-channel μ -GT which thermally reduced at 1200 °C is about $1.99 \times 10^4 \text{ S m}^{-1}$ at room temperature. It is comparable with the graphene-based fiber prepared by CVD method [27], and more than twice

as much as that of the single-channel μ -GTs prepared by electrochemical deposition technique [28].

Despite of the high-temperature annealing, the multi-channel μ -GTs still has a good flexibility because of the highly vertically aligned reduced GO sheets in the tube wall as well as the multiple inner structure. As shown in Fig. 5a and Movie S1, Supporting Information, the LED lamp can be powered by a 6 V dry cell with the conductivity wire of the multi-channel μ -GT thermally reduced at 1200 °C. And the brightness remains stable when the multi-channel μ -GT was bent over and over again on the max bending with an angle of 85°. To further demonstrate the potential application in wearable devices, the bending tests of the electrical properties of multi-channel μ -GT were carried out by measuring their relative resistance changes. The relative resistance shows a negligible variation in either the straight or bent state through an 800-cycle bending test, as shown in Fig. 5b. The excellent electromechanical stability indicates great potential of multi-channel μ -GT in flexible electronics and wearable devices.

Due to the good conductivity, excellent flexibility, and large specific surface area, the multi-channel μ -GT provides an idea platform for post-synthesis through combination of various materials with different properties into the tube bodies for multifunctional applications. As an example, the TiO₂ nanoparticles were intercalated into the framework of reduced GO sheets by soaking the multi-channel μ -GT thermally reduced at 1100 °C in commercial TiO₂ aqueous suspension. The existence of TiO₂ nanoparticles in such systems can be confirmed by its Raman

spectra. As the Raman spectra of TiO₂/multi-channel μ -GT composite shown in Fig. 2b, four extra Raman-active modes with frequencies at 146, 399, 513, and 639 cm⁻¹ obviously appear as well as the two peaks at \sim 1345 cm⁻¹ (D band) and \sim 1580 cm⁻¹ (G band) from the multi-channel μ -GT. These four peaks are unusual characteristics of the anatase [41, 42], which indicates the successful preparation of TiO₂/multi-channel μ -GT composite. The actual test results indicate that there is a fast and uniform photocurrent responding to each switch-on and switch-off event in the TiO₂/multi-channel μ -GT electrode as shown in Fig. 6, which means a direct electron/hole injection between the TiO₂ particles and graphene sheets through photoexcitation of TiO₂ [5, 43, 44], suggesting the important applications in optoelectronic fields.

Conclusions

In summary, the ESD technique was introduced to fabricate the graphene oxide-coated polyester thread from cost-efficient graphene oxide suspensions. Multi-channel μ -GT was successfully prepared after the polyester thread template was removed along with the reduction of GO sheets. The multiple structure within the cross section and vertically aligned reduced GO sheets of the multi-channel μ -GT wall promise many excellent properties, such as highly conductive, good flexibility, and functionalization. The high-performance multi-channel μ -GTs obtained by the sample method open the immense

Figure 5 **a** Digital photograph of the multi-channel μ -GT used as a conductive wire for lighting a LED, the inset is the multi-channel μ -GT under bending with an angle of 85°. **b** Cyclic stability of the multi-channel μ -GT under the repeated bending, the insets are photos of straight (left) and bent (right) multi-channel μ -GT during the test.

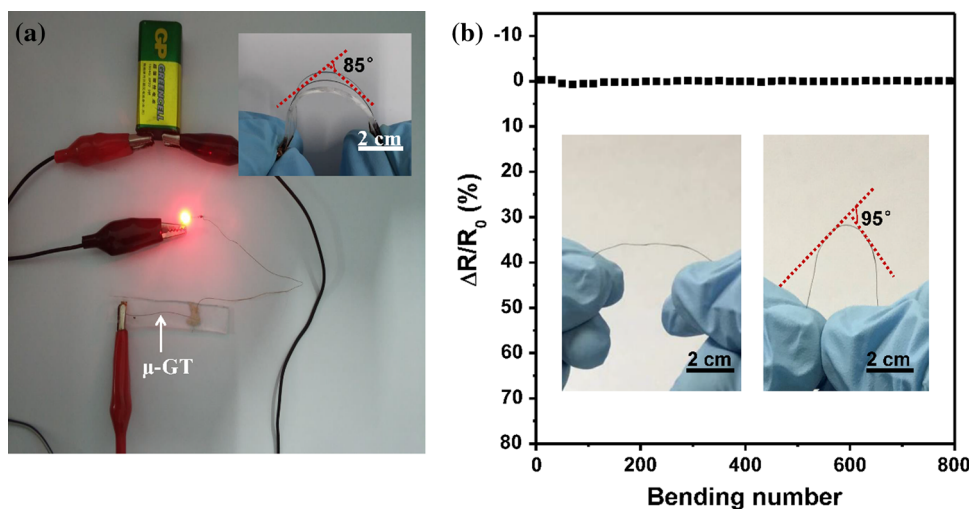
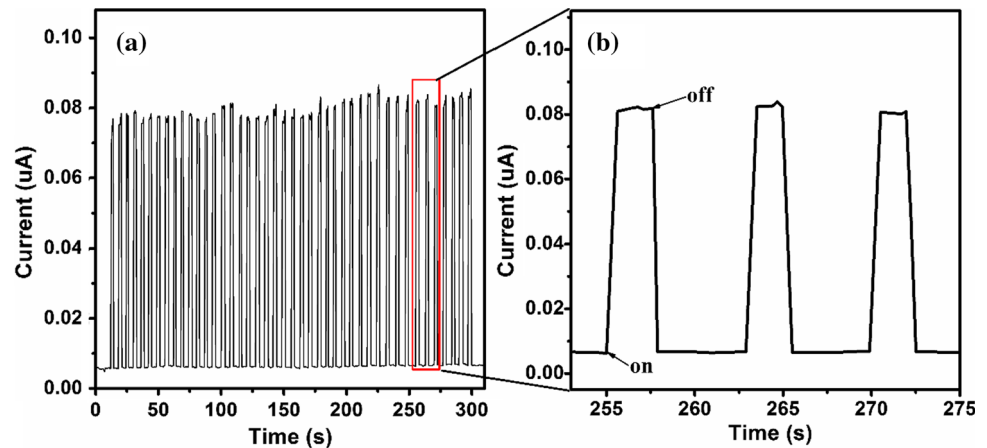


Figure 6 **a** A typical photocurrent response for TiO₂/multi-channel μ -GT electrode exposure to on/off light. **b** An enlarged view for a small section of the photocurrent response curve.



potentials for application in smart clothing and flexible electronics.

Acknowledgements

The authors acknowledge support from National Natural Science Foundation of China (11604173, 51673103 and 11474277), Project of Shandong Province Higher Educational Science and Technology Program (J16LJ07), Project funded by China Post-doctoral Science Foundation (2017M612195), and PT acknowledges support from the Beijing Municipal Science and Technology Commission.

Compliance with ethical standards

Conflict of interest The authors declare no competing financial interest.

Electronic supplementary material: The online version of this article (<https://doi.org/10.1007/s10853-019-03933-7>) contains supplementary material, which is available to authorized users.

References

- Balandin AA, Ghosh S, Bao W, Calizo I, Teweldebrhan D, Miao F, Lau C (2008) Superior thermal conductivity of single-layer graphene. *Nano Lett* 8(3):902–907
- Novoselov KS, Geim AK, Morozov SV, Jiang D, Katsnelson MI, Grigorieva IV, Dubonos SV, Firsov AA (2005) Two-dimensional gas of massless Dirac fermions in graphene. *Nature* 438(7065):197–200
- Novoselov KS, Geim AK, Morozov SV, Jiang D, Zhang Y, Dubonos SV, Grigorieva IV, Firsov AA (2004) Electric field effect in atomically thin carbon films. *Science* 306(5696):666–669
- Lee C, Wei X, Kysar JW, Hone J (2008) Measurement of the elastic properties and intrinsic strength of monolayer graphene. *Science* 321(5887):385–388
- Dong Z, Jiang C, Cheng H, Zhao Y, Shi G, Jiang L, Qu L (2012) Facile fabrication of light, flexible and multifunctional graphene fibers. *Adv Mater* 24(14):1856–1861
- Jang EY, Carretero-González J, Choi A et al (2012) Fibers of reduced graphene oxide nanoribbons. *Nanotechnology* 23(23):235601
- Xu Z, Gao C (2011) Graphene chiral liquid crystals and macroscopic assembled fibres. *Nat Commun* 2:571
- Kwak J, Chu JH, Choi JK et al (2012) Near room-temperature synthesis of transfer-free graphene films. *Nat Commun* 3:645
- Liang M, Wang J, Luo B, Qiu T, Zhi L (2012) High-efficiency and room-temperature reduction of graphene oxide: a facile green approach towards flexible graphene films. *Small* 8(8):1180–1184
- Kim F, Cote LJ, Huang J (2010) Graphene oxide: surface activity and two-dimensional assembly. *Adv Mater* 22(17):1954–1958
- Li X, Cai W, Jinho A et al (2009) Large-area synthesis of high-quality and uniform graphene films on copper foils. *Science* 324(5932):1312–1314
- Wang G, Sun X, Lu F, Sun H, Yu M, Jiang W, Liu C, Lian J (2012) Flexible pillared graphene-paper electrodes for high-performance electrochemical supercapacitors. *Small* 8(3):452–459
- Ye X, Zhou Q, Jia C, Tang Z, Zhu Y, Wan Z (2017) Producing large-area, foldable graphene paper from graphite oxide suspensions by in situ chemical reduction process. *Carbon* 114:424–434
- Li C, Shi G (2012) Three-dimensional graphene architectures. *Nanoscale* 4(18):5549–5563

- [15] Xu Y, Sheng K, Li C, Shi G (2010) Self-assembled graphene hydrogel via a one-step hydrothermal process. *ACS Nano* 4(7):4324–4330
- [16] Bi H, Yin K, Xie X et al (2012) Low temperature casting of graphene with high compressive strength. *Adv Mater* 24(37):5124–5129
- [17] Zhao J, Ren W, Cheng HM (2012) Graphene sponge for efficient and repeatable adsorption and desorption of water contaminations. *J Mater Chem* 22(38):20197–20202
- [18] Xu Z, Sun H, Zhao X, Gao C (2013) Ultrastrong fibers assembled from giant graphene oxide sheets. *Adv Mater* 25(2):188–193
- [19] Xiang C, Young CC, Wang X et al (2013) Large flake graphene oxide fibers with unconventional 100% knot efficiency and highly aligned small flake graphene oxide fibers. *Adv Mater* 25(33):4592–4597
- [20] Li J, Li J, Li L, Yu M, Ma H, Zhang B (2014) Flexible graphene fibers prepared by chemical reduction-induced self-assembly. *J Mater Chem A* 2(18):6359–6362
- [21] Xin G, Yao T, Sun H et al (2015) Highly thermally conductive and mechanically strong graphene fibers. *Science* 349(6252):1083–1087
- [22] Xu Z, Liu Y, Zhao X et al (2016) Ultrastiff and strong graphene fibers via full-scale synergetic defect engineering. *Adv Mater* 28(30):6449–6456
- [23] Kim IH, Yun T, Kim JE et al (2018) Mussel-inspired defect engineering of graphene liquid crystalline fibers for synergistic enhancement of mechanical strength and electrical conductivity. *Adv Mater* 30(40):1803267
- [24] Ma T, Gao HL, Cong HP et al (2018) A bioinspired interface design for improving the strength and electrical conductivity of graphene-based fibers. *Adv Mater* 30(15):1706435
- [25] Zhang Z, Zhang P, Zhang D, Lin H, Chen Y (2018) A new strategy for the preparation of flexible macroscopic graphene fibers as supercapacitor electrodes. *Mater Des* 157:170–178
- [26] Zhao Y, Jiang C, Hu C et al (2013) Large-scale spinning assembly of neat, morphology-defined, graphene-based hollow fibers. *ACS Nano* 7(3):2406–2412
- [27] Chen T, Dai L (2015) Macroscopic graphene fibers directly assembled from CVD-grown fiber-shaped hollow graphene tubes. *Angew Chem* 127(49):15160–15163
- [28] Yang J, Weng W, Zhang Y et al (2018) Highly flexible and shape-persistent graphene microtube and its application in supercapacitor. *Carbon* 126:419–425
- [29] Hu C, Zhao Y, Cheng H et al (2012) Graphene microtubings: controlled fabrication and site-specific functionalization. *Nano Lett* 12(11):5879–5884
- [30] Wang X, Qiu Y, Cao W, Hu P (2015) Highly stretchable and conductive core–sheath chemical vapor deposition graphene fibers and their applications in safe strain sensors. *Chem Mater* 27(20):6969–6975
- [31] Tang H, Yang C, Lin Z, Yang Q, Kang F, Wong CP (2015) Electro-spray-deposition of graphene electrodes: a simple technique to build high-performance supercapacitors. *Nanoscale* 7(20):9133–9139
- [32] Beidaghi M, Wang Z, Gu L, Wang C (2012) Electrostatic spray deposition of graphene nanoplatelets for high-power thin-film supercapacitor electrodes. *J Solid State Electrochem* 16(10):3341–3348
- [33] Xin G, Sun H, Hu T, Fard HR, Sun X, Koratkar N, Borcasciuc T, Lian J (2014) Large-area freestanding graphene paper for superior thermal management. *Adv Mater* 26(26):4521–4526
- [34] Yan J, Leng Y, Guo Y et al (2019) Highly conductive graphene paper with vertically aligned reduced graphene oxide sheets fabricated by improved electro-spray deposition technique. *ACS Appl Mater Interfaces* 11:10810–10817
- [35] Pei S, Cheng HM (2012) The reduction of graphene oxide. *Carbon* 50(9):3210–3228
- [36] Wu JB, Lin M, Cong X, Liu HN, Tan PH (2018) Raman spectroscopy of graphene-based materials and its applications in related devices. *Chem Soc Rev* 47(5):1822–1873
- [37] Díez-Betriu X, Álvarez-García S, Botas C, Álvarez P, Sánchez-Marcos J, Prieto C, Menéndez R, de Andrés A (2013) Raman spectroscopy for the study of reduction mechanisms and optimization of conductivity in graphene oxide thin films. *J Mater Chem C* 1(41):6905–6912
- [38] Pei S, Zhao J, Du J, Ren W, Cheng HM (2010) Direct reduction of graphene oxide films into highly conductive and flexible graphene films by hydrohalic acids. *Carbon* 48(15):4466–4474
- [39] Shin HJ, Kim KK, Benayad A et al (2009) Efficient reduction of graphite oxide by sodium borohydride and its effect on electrical conductance. *Adv Funct Mater* 19(12):1987–1992
- [40] Li X, Zhang G, Bai X, Sun X, Wang X, Wang E, Dai H (2008) Highly conducting graphene sheets and Langmuir–Blodgett films. *Nat Nanotechnol* 3(9):538–542
- [41] Dai Y, Jing Y, Zeng J et al (2011) Nanocables composed of anatase nanofibers wrapped in uv-light reduced graphene oxide and their enhancement of photoinduced electron transfer in photoanodes. *J Mater Chem* 21(45):18174–18179
- [42] Liang D, Cui C, Hu H et al (2014) One-step hydrothermal synthesis of anatase TiO₂/reduced graphene oxide nanocomposites with enhanced photocatalytic activity. *J Alloys Compd* 582:236–240
- [43] Zou F, Yu Y, Cao N, Wu L, Zhi J (2011) A novel approach for synthesis of TiO₂–graphene nanocomposites and their photoelectrical properties. *Scripta Mater* 64(7):621–624

- [44] Zhang Y, Pan C (2011) TiO₂/graphene composite from thermal reaction of graphene oxide and its photocatalytic activity in visible light. *J Mater Sci* 46(8):2622–2626. <https://doi.org/10.1007/s10853-010-5116-x>
- [45] Park S, Lee KS, Bozoklu G, Cai W, Nguyen ST, Ruoff RS (2008) Graphene oxide papers modified by divalent ions—enhancing mechanical properties via chemical cross-linking. *ACS Nano* 2:572–578

Publisher's Note Springer Nature remains neutral with regard to jurisdictional claims in published maps and institutional affiliations.